J Mol Hist (2015) 46:157–171
DOI 10.1007/s10735-014-9608-x

ORIGINAL PAPER

Downregulation of angiogenin inhibits the growth and induces apoptosis in human bladder cancer cells through regulating AKT/mTOR signaling pathway

Jing Shu · Mengge Huang · Qiang Tian · Qinglin Shui · Yujian Zhou · Junxia Chen

Received: 11 November 2014 / Accepted: 30 December 2014 / Published online: 7 January 2015

Abstract Angiogenin (ANG) is a multifunctional secreted protein that belongs to the pancreatic ribonuclease A super family, which has been conceived to play a more important role in cell survival, growth and proliferation than the mediation of angiogenesis. Accumulating evidences suggest that the expression and activity of ANG increased significantly in a variety of human cancers. Recent studies showed that ANG activates cell signaling pathway through the putative receptor on endothelial cells. However, the underlying mechanisms remain largely unknown. AKT/mTOR signaling pathway participates in cell growth, cell-cycle progression and cell apoptosis. The purpose of our study was to determine whether ANG implicated in growth and metastasis of bladder cancer cells through regulating AKT/mTOR signaling pathway. In this study, we constructed ANG siRNA plasmids that transfected into human bladder cancer T24 cells. We demonstrated that knockdown of ANG could inhibit cell proliferation, regulate cell cycle and induce apoptosis. We also found that down-regulation of ANG remarkably reduced the phosphorylation of signaling targets AKT, GSK-3β and mTOR. Furthermore, down-regulation of ANG increased expression of ribonuclease inhibitor, which is a cytoplasmic acidic protein with many functions. Finally, ANG siRNA led to the suppression for tumorigenesis and metastasis in vivo. Taken together, these findings highlight for the first time that ANG could play a pivotal role in the development of bladder cancer through regulating AKT/mTOR signaling pathway. The targeting of ANG and associated factors could provide a novel strategy to inhibit human bladder cancer.

Keywords Angiogenin · Apoptosis · Bladder cancer cells · AKT/mTOR signaling pathway

Introduction

The bladder cancer is a very common malignant tumor at the urinary system with significant associated morbidity and mortality. Globally it is the ninth most common cause of cancer related death in men, the overall incidence of bladder cancer has increased by approximately 40 % in recent decades, and the prognosis for patients with high-risk or advanced metastatic bladder cancer remains poor, five-year survival rates are around 50 % (Jemal et al. 2011; Suriano et al. 2013). Angiogenin (ANG), a single chain of alkaline protein of 14.4 KD originally isolated from the conditioned medium of HT-29 human colon adenocarcinoma cells (Fett et al. 1985), has been shown to play important role in tumor angiogenesis. More importantly, ANG is implicated in a wide range of biological functions including cell survival, growth, proliferation, migration, tube formation and tumor angiogenesis (Yuan et al. 2009;

Jing Shu, Mengge Huang have contributed equally to this work.

J. Shu · J. Chen (✉)
Department of Cell Biology and Genetics, Chongqing Medical University, Chongqing 400016, People's Republic of China
e-mail: chjunxia@126.com

M. Huang
Department of Clinical Medicine, Luzhou Medical College, Luzhou 646000, Sichuan, People's Republic of China

Q. Tian · Q. Shui
Department of Cell Biology and Genetics, Luzhou Medical College, Luzhou 646000, Sichuan, People's Republic of China

Y. Zhou
The Experimental Teaching Center, Chongqing Medical University, Chongqing 400016, People's Republic of China

Ivanov et al. 2011; Li and Hu 2012). Recent research demonstrated that ANG expression and activity were up-regulated significantly in a variety of human tumors including breast, lung, colorectal, kidney and pancreatic cancers, and the increases are correlated with tumor progression and poor prognosis in patients (Yoshioka et al. 2006; Nilsson et al. 2010). Trouillon et al. reported that ANG activated nitric oxide synthase (NOS) by interacting with the cell nucleus. Similarly, NOS activity was stopped by blocking the PI-3K/Akt kinase signaling transduction cascade, showing the importance of this pathway and ANG for NOS activity (Trouillon et al. 2010). Kim, et al. demonstrated that ANG induces transient phosphorylation of protein kinase B/Akt in cultured human umbilical vein endothelial (HUVE) cells (Kim et al. 2007). ANG is upregulated in human prostate cancer and is the most significantly upregulated gene in AKT-driven prostate intraepithelial neoplasia (PIN) in mice. ANG has been shown to activate Akt (Ibaragi et al. 2009a, b). The results suggest that cross-talk between ANG and protein kinase B/Akt signaling pathways could be essential for ANG -induced angiogenesis and other biological function (Kieran et al. 2008). This crosstalk between ANG and AKT may thus coordinate an orchestrated synthesis of ribosomes. Ribosome biogenesis requires both ribosome proteins and rRNAs. The production of ribosomal proteins is mediated by the AKT-mTOR pathway. The AKT/mTOR signaling pathway is thought to be a central mediator in signal transduction pathways, which is frequently activated in diverse cancers (Janku et al. 2013). The AKT/mTOR signaling regulates cell proliferation, differentiation, cellular metabolism, apoptosis and cancer cell survival (Liu et al. 2009; Janku et al. 2012). However, the signal transduction pathway triggered by ANG-receptor interaction is currently unclear as the identity of a functional ANG receptor has not been fully determined (Li and Hu 2010). Lately, the reports showed that ANG concentration was increased in the urine of patients with bladder cancer (Rosser et al. 2013; Urquidi et al. 2012). So far, whether ANG plays a significant role in development of bladder cancer and its biological mechanisms remain fully unknown.

Therefore, we presumed that AGN might be involved in growth and metastasis of bladder cancer through regulating AKT/mTOR signaling pathway. Here, we found that down-regulating ANG not only changed cell morphology, but also inhibited cell proliferation and induced apoptosis in bladder cancer cells. Moreover, the data also showed that ANG knockdown could dramatically inhibit tumor growth and metastasis through suppressing AKT/mTOR signaling pathway. In summary, our findings demonstrated for the first time that ANG play a crucial role in tumor development of bladder cancer cells via the AKT/mTOR signaling pathway. ANG might be useful as a potential therapy target for human bladder cancer.

Materials and methods

Cell lines, animal and reagents

T24 cells and pGensil-1siRNA plasmid were prepared by our laboratory. BALBC nude (nu/nu) mice were purchased from the Peking University Laboratory Animal Center (Beijing, PR China). Mice were maintained according to National Institutes of Health standards for the care and use of experimental animals. The protocol was approved by The Ethics Committee of Chongqing Medical University. Fetal calf serum was bought from Hyclone (Logan, Utah, USA). RPMI 1640 medium and G418 were from Gibco-BRL (Carlsbad, CA, USA). Lipofectamine 2000 reagent and Trizol were bought from Invitrogen, Inc. (Carlsbad, California, USA). Polyclonal rabbit anti-human RI antibody was prepared by our laboratory, rabbit anti- human β-actin and CD31 antibodies were purchased from Santa Cruz Biotechnology (Santa Cruz, CA, USA). Monoclonal mouse anti-human AGN antibody, rabbit anti-human antibody of Bcl-2, Bax, Caspase3, p-Akt, Akt, p-mTOR, mTOR, 4E-BP1, p70 S6 Kinase, p-4E-BP1, p-p70 S6 Kinase, GSK3(α/β), p-GSK3β were bought from Bioworld Technology, Inc (St. Louis, USA). The rest of the primary antibodies are from Beijing Zhongshang Biotechnology (Beijing, PR China).

ANG siRNA plasmid construction

Human ANG cDNA sequence (Accession number: NM_000014.8) were provided by the GenBank. Appropriate sense strands of oligonucleotides that target the ANG mRNA siRNA were designed using ambion online siRNA finder (www.ambion.com). A random, with no homology to the human sequence was used as control; it contains the same oligonucleotides with ANG siRNA. ANG siRNA expressed plasmids were constructed as follows: ANG siRNA forward and reverse:

- 5′-GATCCGGAATGGAAACCCTCACAGATTCAAGAGATCTGTGAGGGTTTCCATTCTTTTTTGTCGACA-3′
- 3′-GCCTTACCTGGGAGTGTCTAAGTTCTCTAGACACTCCCAAAGGTAAGAAAAAACAGCTGTTCAG-5′

ANG siRNA control forward and reverse:

- 5′-GATCCGCGCAGAAAACGAGACACGAGATTCAAGAGATCTCGTGTCTCGTTTTCTGCGTTTTTTGTCGACA-3′

- 3′-GCGCGTCTTTTGCTCTGTGCTCTAAGTTCTCT AGAGCACAGAGCAAAAGACGCAAAAAACAGCT GTTCGA-5′

Annealed double-stranded oligonucleotides were connected into the pGenesil-1 plasmid. All recombinant plasmids were identified by endonuclease sal I digestion. Finally they were further verified by DNA sequencing. Subsequent analysis was performed using BLAST software (available on the World Wide Web at ncbi.nlm.nih.gov/blast/).

Cell culture and gene transfection

The T24 cells were maintained in RPMI 1640 medium supplemented with 10 % fetal calf serum at 37° C in a 5 % CO_2 incubator. Before transfection, cells were seeded into six well plates at a density of 2×10^5 per well until the cells reached about 70 % confluence, and transfected with the plasmids using Lipofectamine 2000 reagent according to the manufacturer's instructions. The cells were divided into the following three groups: T24-siANG cells, T24-vector cells and T24 cells. 48 h after transfection, the selection was performed with 800 μg/ml concentrations of G418 for 14 days and 400 μg/ml concentrations of G418 for additional 14 days. The individual G418-resistant monoclines were obtained by limiting dilution, then proliferated and expanded to generate stable transfected cell lines.

RT-PCR analysis

The total RNA was isolated from cells using the Trizol reagent according to manufacturer's instruction (Invitrogen). Reverse transcription was performed and cDNAs were amplified with the following primer pairs, ANG forward: 5′-CAGCACTATGCCAAACCAC-3′ and reverse: 5′-GA AATGGAAGGCAAGGACAGC-3′; GAPDH of the same sample was used as an internal control, GAPDH forward: 5′-GCTGTCCCTGTACGCCTCTG-3′ and reverse: 5′- TGCC GATGGTGATGACCTGG-3′. RT-PCR was performed under the following conditions: 37 °C for 15 min, 85 °C for 5 s for RT reaction, then 94 °C for 2 min, 94 °C for 30 s, 58 °C for 30 s and 72 °C for 30 s and a total of 30 cycles, then a final extension of 72 °C for 10 min. The PCR products were separated on 2 % agarose gel, stained with Gold-View, photographed under UV. Results were collected and analyzed by using Quantity One software from Bio-Rad. Experiments were performed in triplicate and repeated three times.

Quantitative real-time PCR

The total RNA was isolated from cells using the Trizol reagent according to manufacturer's instruction (Invitrogen), and reverse transcribed into cDNA. Real-time PCR was performed with an ABI 7400 System using the TaqMan EZ RT-PCR kit according to the manufacturer's protocol. TaqMan primers and probes were derived from the commercially available TaqMans Assays-on-Demand Gene Expression Products. We selected GAPDH as the endogenous control for the real-time PCR relative quantification analysis. PCR cycling conditions were as follows: initial incubation step of 2 min at 50 °C, reverse transcription of 60 min at 60 and 94 °C for 2 min, followed by 40 cycles of 15 s at 95 °C for denaturation and 2 min at 62 °C for annealing and extension. PCR was run using the SYBR GREEN PCR kit. The primers for ANG were 5′-CAG GAT AAC TCC AGG TAC-3′ and 5′-CGG ACG ACG GAA AAT TG-3′; The primers for the internal control gene GAPDH were 5′-ACG GAT TTG GTC GTA TTG GG-3′ and 5′-CGC TCC TGG AAG ATG GTG AT-3′. Each sample was run in triplicate. Average threshold cycle (Ct) values for ANG was normalized against the average Ct values for GAPDH from the same cDNA sample and calculation of relative mRNA level was based on the cycle threshold method.

Western blotting assay

The cells were washed three times with ice-cold PBS (pH 7.4). Cells total proteins were extracted using lysis RIPA buffer, protein concentration was measured by Enhanced BCA Protein Assay Kit. Equal amounts (30 μg) of protein were loaded into each lane and separated by 10 % SDS-PAGE gel electrophoresis, and then were electrotransferred to a PVDF membrane at 200 mA for 2 h. Next, the samples were blocked in TBST buffer (0.1 % Tween 20, 150 Mm NaCl, and 10 mmol/l Tris–HCl, pH 7.6) containing 5 % skimmed milk powder at normal temperature for 1 h to block non-specific antibodies. Then they were incubated in antibodies against RI (1:200 dilution), ANG (1:250 dilution), Bcl-2 (1:500 dilution), Bax (1:500 dilution), Caspase 3 (1:1,000 dilution), AKT (1:500 dilution), p-AKT (1:500 dilution), p-GSK3β (1:500 dilution), GSK3(α/β) (1:500 dilution), p-mTOR (1:500 dilution), mTOR (1:500 dilution) and β-actin (1:1,000 dilution) overnight at 4 °C, washed 3 × 10 min with TBST, and incubated with goat anti-rabbit secondary antibody (1:1,000 dilution) respectively for 1 h at 37 °C, washed thoroughly 3 × 10 min with TBST. The bands were detected by enhanced chemiluminescence method (BeyoECL Plus). Results were collected and analyzed with MJ Opticon Monitor Analysis Software (Bio-Rad). Experiments were performed in triplicate and repeated three times.

Immunofluorescence and laser scanning confocal detection

Cells were seeded on cover slips in 24 well plates for 24 h and washed three times with PBS, fixed with ice-cold 4 %

paraform phosphate buffer saline for 20 min, the coverslips were treated with 3 % BSA in PBS for 30 min at 37 °C to block non-specific antibodies. The samples were incubated in the monoclonal primary antibody mouse anti-human ANG (1:150 dilution), rabbit anti-human p-Akt (1:200 dilution), p-GSK3β (1:200 dilution), p-mTOR (1:150 dilution), as well as the polyclonal antibody rabbit anti-human RI (1:200 dilution) overnight at 4 °C. After washed three times with PBS, cells were incubated with DyLightTM 594-Conjugated Goat Anti-Mouse IgG secondary antibody (1:100 dilution), Rhodamine (TRITC)-Conjugated Goat Anti-Rabbit IgG secondary antibody (1:100 dilution) respectively for 1 h at 37 °C in the dark, washed thrice with PBS for 5 min, and finally sealed with 50 % glycerin. Observations were performed under Olympus multifunction microscope and laser scanning confocal microscope (Leica TCS-SP2, German).

Cell morphology and cell proliferation

Cells were grown on cover slips in 6-well plates for 24 h and washed with PBS for 3 × 5 min, then were fixed by absolute alcohol for 15 min and washed 3 × 5 min with PBS and stained with HE. Finally, their images were captured under phase contrast inverted microscope (NIKON TE2000-U, Japan). The T24 cells proliferation was detected every 24 h by MTT assay. An amount of 3×10^3 cells per well were seeded into 96 wells plates with 150 μl medium and incubated at 37°Cin a 5 % CO_2 humidified incubator. The plates were further incubated at 37 °C for 4 h after MTT of 20 μl (5 mg/ml) was added into each well, the medium was removed and each well was supplied with 150 μl DMSO and then the absorbance was measured with a plate reader at 490 nm. Each point represents the mean of 6 independent samples and assay was repeated three times.

The cell cycle assay

The cells were washed with PBS and counted; each sample contained 2×10^6 cells. Cells were fixed for 12 h in 70 % ethanol, then collected and washed with PBS for three times. Cells were stained with propidium iodide (PI) and incubated in dark at 4 °C for 30 min. The cell cycle phase distribution was analyzed by flow cytometry (Becon Dickinson FACSCalibur, USA). Experiments were repeated three times.

Apoptosis detection

The cells were seeded on cover slips in six well plates for 24 h. The cover slips were washed with PBS. The cells was fixed in 4 % paraform phosphate buffer saline for 30 min, washed with PBS, and then were dyed with Hoechst 33342 (8 μg/ml) in the dark for 10 min, and washed with PBS. Finally, the observation was performed under Olympus multifunction microscope (Tokyo, Japan). TdT-UTP nick end labeling (TUNEL) assays were detected with the one step TUNEL kit according to the manufacturer's instructions. Briefly, the cells was fixed with 4 % paraform phosphate buffer saline for 30 min, rinsed with PBS, treated with 0.1 % Triton X-100 for 2 min on ice, incubated with TUNEL for 1 h at 37 °C. The FITC-labeled TUNEL-positive cells were imaged under a fluorescent microscope. The cells with green fluorescence were recognized as apoptotic cells. The cells were collected and double stained with fluorescein isothiocyanate (FITC)-conjugated Annexin V and PI apoptosis detection kit (Beckman Coulter). The cell apoptosis were analyzed by flow cytometry (Becon Dickinson FACSCalibur, USA). Experiments were performed in triplicate.

Tumor xenograft and spontaneous metastasis model

Each group of cells was collected at a density of 2×10^5 and 0.1 ml of the cell suspensions were respectively injected into the back of each nude mouse BALB/C (8–12 weeks old, SPF degree, 20 ± 3 g). Each group contained eight mice. The time of tumor formation was recorded, 4 weeks after injection, all the mice were sacrificed. The tumors were removed and weighed. Then, a part of the tumors tissue were fixed in 10 % buffered formalin with for pathology analysis, the others were quickly placed in liquid nitrogen for frozen section of immunofluorescence assay. The inhibitory rate of tumor was calculated by the following formula: inhibitory rate = (tumor weight of T24 control group − tumor weight of T24-siANG group)/ tumor weight of T24 control group × 100 %.

Histology, immunofluorescence and immunohistochemistry assay of tumor tissue

Tumors and lungs were fixed in 10 % buffered formalin and embedding in paraffin, and sections of 5 μm thick were stained with hematoxylin-eosin (HE). The microvessels were counted from 10 different fields under microscope (×200) corresponding to areas with the highest density of vessels. As mentioned above immunofluorescence assays. The tumor frozen tissue sections were incubated overnight in primary antibodies of ANG, RI, p-AKT, p-GSK3β, p-mTOR, p-4E-BP1, p-p70 S6 Kinase and CD31 (1:200 dilution) at 4 °C respectively. After they were washed with PBS for 3 × 5 min, incubated with Rhodamine (TRITC)-Conjugated Goat Anti-Rabbit IgG or FITC-Conjugated Goat Anti-Rabbit IgG (1:100 dilution) for 1 h at 37 °C in the dark, washed again with PBS for 3 × 5 min, and finally

sealed with 50 % glycerin. Observations were performed by Olympus multifunction microscope (Tokyo, Japan). Immunohistochemistry assays for ANG, RI, Bcl-2, Bax, Caspase3, AKT, p-AKT, GSK3β, p-GSK3β, mTOR, p-mTOR, 4E-BP1, p-4E-BP1, p70 S6 Kinase and p-p70 S6 Kinase were done to detect the impact of ANG expressions on apoptosis and PI3K/AKT/mTOR signaling pathway. The antigen retrieving steps were taken in the citrate buffer for 30 min at 95 °C in the microwave oven. Tissue sections were incubated overnight in primary antibodies (1:200 dilution) at 4° C respectively, then the secondary antibodies incubating in goat anti-rabbit or goat anti-mouse IgG for 30 min at 37 °C by SP (Streptavidin/Peroxidase) Histostain TM-Plus Kits and diaminobenzidine (DAB) staining. The nuclei were counterstained by hematoxylin. The rest of the procedure was carried out according to manufacturer's instruction.

Statistical analysis

All data were dealt with SPSS18.0 statistical software. The values were expressed as mean ± SD. Student's t tests were used for statistical analysis. P values of < 0.05 were considered to be significant.

Results

ANG siRNA expression is identified and ANG siRNA affects RI expression

ANG siRNA expression vectors were constructed and identified with endonuclease digesting and DNA sequencing, two bands, about 400 and 4,400 bp were generated after Sal I digestion (data not shown); the DNA sequencing results also indicated identical nucleotide sequence with the design (data not shown), which confirmed the correct construction of plasmids. Forty-eight hours after transfection, the transfection efficiency was detected under fluorescence microscope. A large number of cells illuminated bright green fluorescence, which represented the high transfection efficiency, but none green fluorescence was detected in non-tansfected cells (Fig. 1a). The transfected cells were isolated by G418 selection, and then cloned, expanded, finally identified by RT-PCR, Western Blot and RT-qPCR. As showed in Fig. 1b–f, the expression of ANG mRNA obviously decreased by 41 or 38 % in T24-siANG cell group and protein levels were significantly reduced by 49 or 53 % in T24-siANG cell group, compared with the other two control cell groups respectively. While the RT-qPCR result showed that T24-siANG cell group led to about 47 % decrease of ANG level compared with control. Laser scanning confocal assay was to used to explore the expression of RI after down-regulation ANG and their colocalizing relationship. The results demonstrated that ANG and RI colocalized in cytoplasm and the expression of RI in T24-siANG cell group markedly increased, compared with the control cells (Fig. 1g).

ANG siRNA affects cell morphology, proliferation, cell cycle

We examined the effects of ANG siRNA on the morphology and proliferation. HE staining showed that the transfected T24-siANG cells became lower malignant phenotype including less overlapping growth, a smaller nucleus, and weaker alkalophilic quality of cytoplasm compared with the other two control groups cells (Fig. 2a); The cell proliferative ability was determined by MTT assay, the 490 nm absorbance is directly proportional to the number of living cells, the A490 was significantly reduced with MTT in the T24-siANG cell group. The T24-siANG cell group showed remarkable lower cell proliferation than those of the T24 and the vector cells groups. The inhibitory rate of T24-siANG cells to T24 vector cells was 0, 10.6, 15.62, 27.5, 33.45 % at 24, 48, 72, 96, 120 h, respectively, $P < 0.05$ (Fig. 2b). Flow cytometry detection of cell cycle profile was performed. The data showed that the G_1 phase was increased from 44.18 ± 1.63 % in T24 cells or 50.44 ± 8.39 % in T24 vector cells to 60.65 ± 6.18 % in T24-siANG cells; The S phase was decreased from 44.71 ± 2.41 % in T24 cells or 42.31 ± 1.51 % in T24 vector cells to 31.12 ± 5.81 % in T24-siANG cells, and The G_2-M phase was decreased from 11.11 ± 1.01 % in T24 cells or 11.21 ± 1.67 % in T24 vector cells to 8.23 ± 0.83 % in T24-siANG cells respectively (Fig. 2c, d). The results demonstrated that the proliferations of T24-siANG cells were inhibited with G_1 phase arresting, S phase and G_2-M reducing, $P < 0.05$.

ANG siRNA induces apoptosis of bladder cancer cells

TUNEL assay, the Hoechst 33342 staining and flow cytometry analysis were undertaken to detect the effect of siRNA ANG on apoptosis. The number of TUNEL-positive cells significantly increased in the T24-siANG cell group, compared with control cells (Fig. 3a). The Hoechst 33342 staining results showed that T24-siANG cell group represented typical apoptotic morphology features such as nuclear shrinkage, chromatin condensation, the nuclear fragmentation, the apoptotic body and brighter blue fluorescent. However, the control cells did not reveal apoptotic characteristics (Fig. 3b). In addition, flow cytometry analysis shown in Fig. 3c, d. About 46.5 % of counted cells became apoptotic in T24-siANG cells group, but apoptotic cells were only 13 and 15 % in T24 and T24 vector cells groups, $P < 0.01$. To further verify the molecular basis of

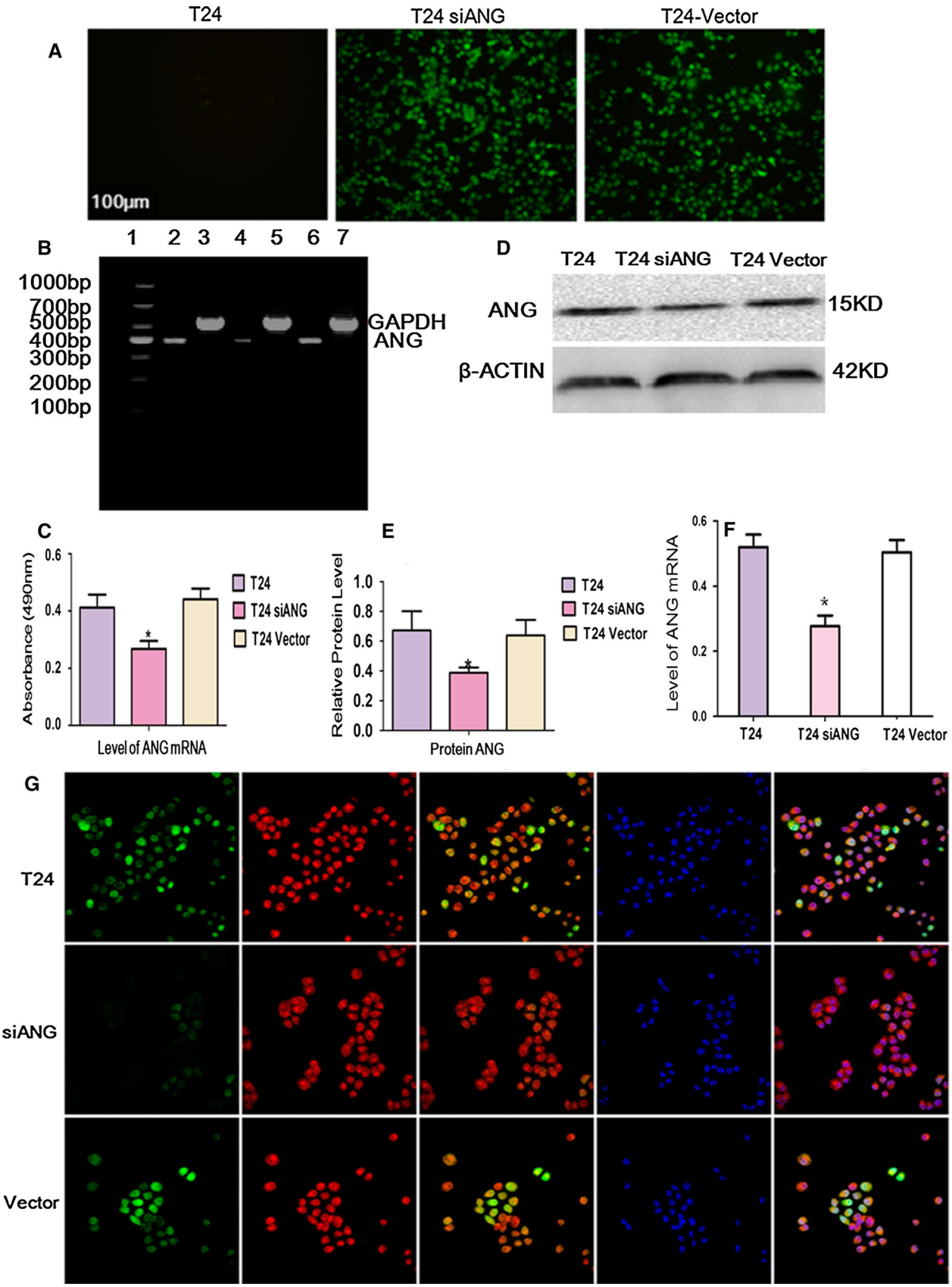
A
T24
T24 siANG
T24-Vector
100μm
B
1 2 3 4 5 6 7
1000bp
700bp
500bp
400bp
300bp
200bp
100bp
GAPDH
ANG
D
T24 T24 siANG T24 Vector
ANG
15KD
β-ACTIN
42KD
C
Absorbance (490nm)
T24
T24 siANG
T24 Vector
Level of ANG mRNA
E
Relative Protein Level
T24
T24 siANG
T24 Vector
Protein ANG
F
Level of ANG mRNA
T24
T24 siANG
T24 Vector
G
T24
T24 siANG
T24 Vector

◀**Fig. 1** siRNA ANG expression and the colocalization of ANG with RI are assayed. **a** The transfection effciency after transfection 48 h by Fluorescence microscopy. The results showed that recombinant pGenesil-1 plasmids have high transfection efficiency in T24-siANG and T24 vector cell groups (×200 magnification). **b**, **c** Analysis of ANG mRNA expression level with RT-PCR. *Lane 1*: marker of 1,000 bp, *Lane 2, 3*: T24 cells; *Lane 4, 5*: T24-siANG cells; *Lane 6, 7*: T24 vector cells. **d**, **e** Determination of ANG protein expression level with Western blot. **f** Analysis of ANG mRNA expression level with RT-qPCR. GAPDH and β-actin were used as internal control in RT-PCR, RT-qPCR and Western blot respectively. The levels of ANG mRNA and proteins were obviously decreased by treatment with siRNA ANG compared with the control groups, $*P < 0.05$. **g** Immunofluorescence staining of RI (*red*) and ANG (*green*) in three kinds of T24 cells with laser scanning confocal microscope. The nucleus was counterstained with DAPI (*blue*). The merge images (*yellow*) demonstrated that ANG with RI colocalized in cells. The expression of RI was increased in T24 siANG cells when compared to the control cells (×200 magnification). (Color figure online)

the apoptosis in T24 cells after down-regulation of ANG, the expressions of apoptosis-related proteins were detected by western blotting. The results showed that Bcl-2 was significantly decreased by 41.47 %, and that the pro-apoptotic expressions of Bax were evidently increased by 54.75 % in the T24-siANG cells, compared with the other two control cells, respectively. Meanwhile, siRNA ANG increased the cleavage of procaspase-3 by 37.19 % in T24-siANG cells group, $*P < 0.05$ (Fig. 3e, f).

ANG siRNA affects RI and PI3K/AKT/mTOR signaling pathway molecules expressions in vivo and in vitro.

In order to confirm the molecular mechanism of the inhibition of cell proliferation after down-regulating ANG, we determined the protein levels of RI and the important signaling pathway target molecules of AKT/mTOR by immunofluorescence and western blot. Then, semi-quantitative analyses of the protein levels were performed. Immunofluorescence assay revealed that T24-siANG group resulted in a much higher RI and lower ANG expression as well as a weaker fluorescent signal of p-Akt, p-GSK3β and p-mTOR, compared with the other two control cells groups respectively in vivo and in vitro. As shown in (Fig. 4a, b) Western blot assay indicated that the expressions of ANG, p-Akt, p-GSK3β and p-mTOR were significantly decreased by 50.14, 47.81 and 55.46 %, respectively, as well as the protein level of RI was increased by 34.14 %, whereas the expression of Akt, GSK3(α/β) and mTOR showed no difference among groups (Fig. 4c, d). Results were consistent with immunofluorescence analysis. The data strongly suggest that down-regulating ANG may be associated with suppression of PI3K/AKT/mTOR signaling pathway.

ANG siRNA inhibits tumor growth and lung metastasis in mouse xenograft model

To study whether ANG had an impact on growth and metastasis of tumor, 2×10^5 cells in 0.1 ml were implanted into the backs of BALB/C nude mice. The

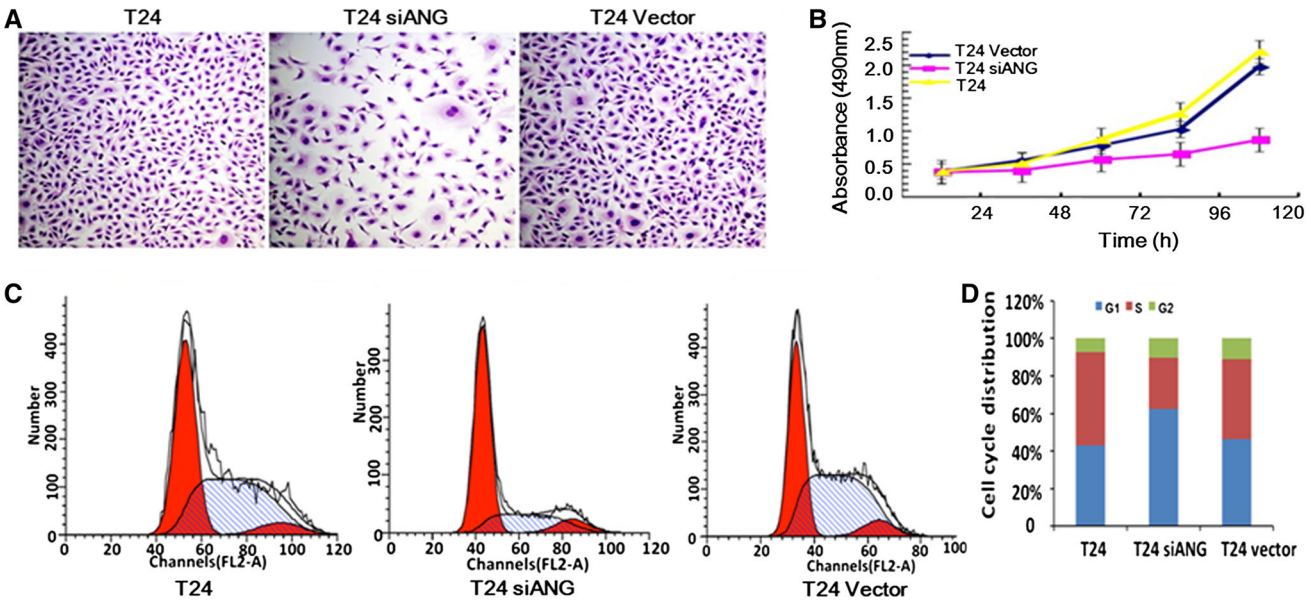

Fig. 2 Effects of siRNA ANG on cell morphology, proliferation, cell cycle are assayed. **a** HE staining of T24, T24-siANG and T24 vector cell groups. The siANG group's cells showed an epithelial morphology, less division phases and weaker alkalophilic quality of cytoplasm compared with some cells in the other control groups. **b** MTT cellular proliferation assays ($*P < 0.05$). 3×10^3 cells were seeded into a 96 well plates, the MTT assay was carried out and recorded the A490 nm absorbance value with a plate reader every 24 h. Each point represents the mean of eight independent samples. Experiments were repeated three times, $P < 0.05$. **c** Flow cytometry images with propidium iodide staining were performed. Experiments were repeated three times. **d** Flow cytometry analysis of cell cycle distribution. The results demonstrated that the proliferation of T24-siANG cells was inhibited with G_1 phase arresting, S phase and G_2-M reducing, $P < 0.05$

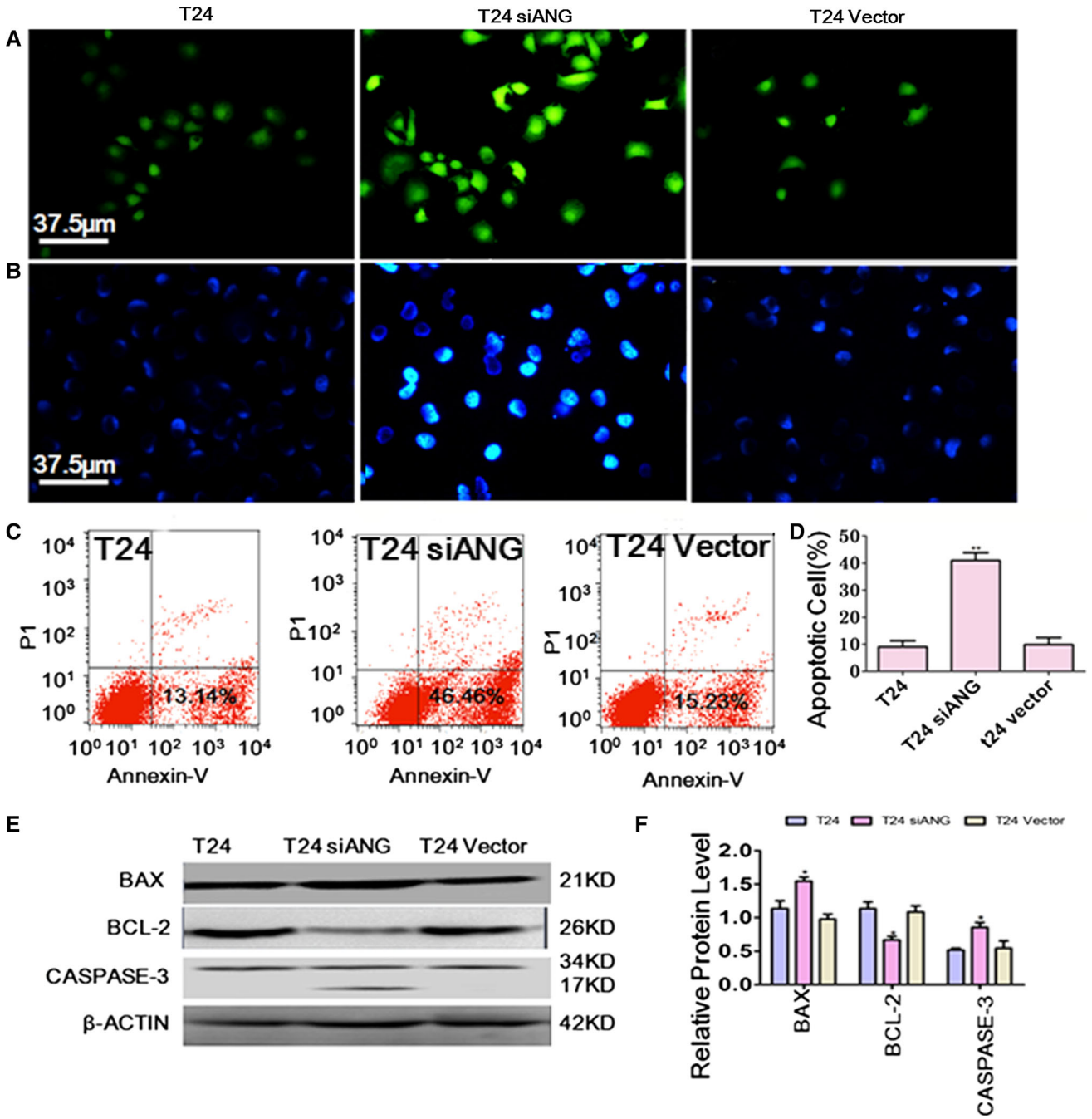

Fig. 3 Down-regulating ANG induces apoptosis of T24 cells. **a** Representative photographs of TUNEL staining of cells were observed. The FITC-labeled TUNEL-positive cells were imaged under a fluorescent microscope (×200 magnification). The cells with *green* fluorescence were recognized as apoptotic cells. **b** The typical photographs of Hoechst 33342 staining were taken (×400 magnification). Some nuclei of T24-siANG cells represented typical morphology of the apoptotic cell as described in Sect. 3, compared with the control group cells. **c**, **d** Flow cytometry analysis with Annexin V/PI staining was performed to evaluate the number of apoptotic cells. Representative images from flow cytometry analysis were shown. The percentages of apoptotic cells in T24-siANG cells group significantly increased than those of control cells respectively, Data were expressed as mean ± S.D. (n = 3), $^{**}P < 0.01$ as determined by Student's *t* test. **E**, **f** Effects of down-regulating ANG on apoptosis-related proteins were detected. BCL-2, BAX and CASPASE-3 were examined by Western blot and Semi-quantitative analysis as described in Sect. 2. β-actin was used as a loading control. Levels of total Caspase 3 did not change significantly, however activated Caspase-3 and Bax remarkably increased as well as Bcl-2 decreased in T24-siANG cells compared with the control cells respectively. Data were expressed as mean ± SD (n = 3), ($^{*}P < 0.05$). (Color figure online)

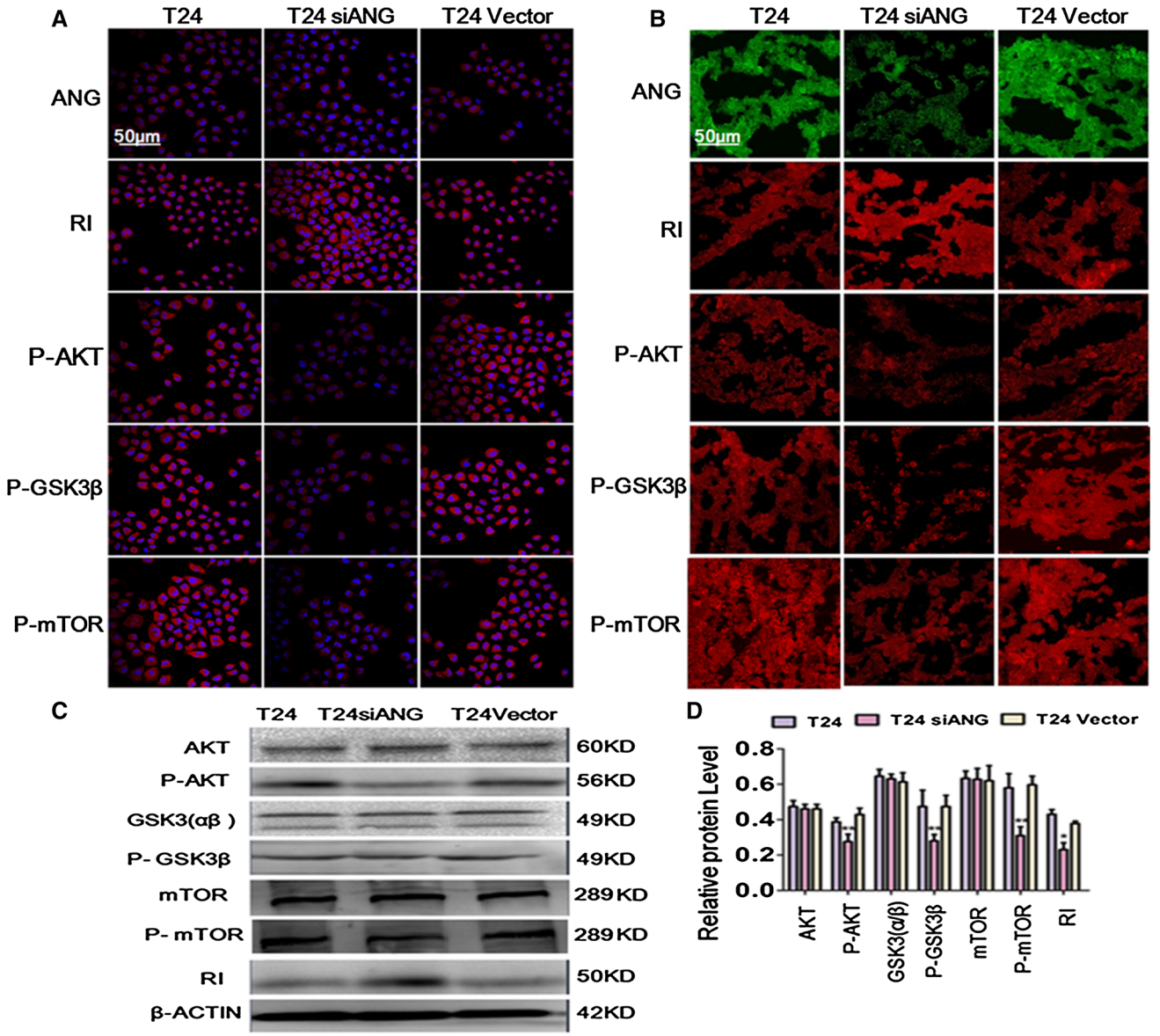

Fig. 4 Effects of down-regulating ANG on the expressions of AKT/mTOR signaling pathway target molecules in vitro and in vivo were determined. **a**, **b** Immunofluorescent observation in cells and tumor tissue. The results revealed that p-Akt, p-GSK3β and p-mTOR were obviously reduced as well as RI was significantly stronger in T24-siANG cells group compared with the other control groups respectively in vitro and in vivo. **c**, **d** AKT, p-AKT, GSK3(α/β), p- GSK3β, mTOR, p-mTOR and RI were examined by Western blot and Semi-quantitative analysis, β-Actin was used as a loading control. Data were expressed as mean ± SD (n = 3), (*$P < 0.05$, **$P < 0.01$). The results showed that T24-siANG cells group remarkably down-regulated the expressions of p-Akt (S473), p-GSK3β (S9), p-mTOR respectively and up-regulated the expressions of RI, but the protein expressions of AKT, GSK3(α/β) and mTOR did not change obviously, compared with control group cells respectively

results showed that the T24-siANG cell group significantly inhibited the growth of bladder cancer compared with the other control groups. The inhibiting rates of tumors were 42.15 and 50.26 % compared with the T24 and T24 vector cells groups (Fig. 5a, b). To identify whether ANG is correlated with the new blood vessel formation, micro-vessels were counted from 10 different fields corresponding to areas with the highest density of vessels on HE sections under a microscope (Fig. 5c, d). The siANG groups showed less vessels compared to the other control groups (*$P < 0.05$). Mice injected with the T24-siANG cells also showed a significant suppression of the spontaneous lung metastasis, which no metastasis was observed in T24-siANG cell groups, whereas lung metastases were detected in all mice of control groups on the HE sections (Fig. 5e). Immunofluorescent analyses of CD31 were also further performed. T24-siANG group showed low CD31 expression and remarkable inhibition of angiogenesis in

tumor tissue; whereas intense CD31 expression and more vessels were seen in tumor tissue of the control groups (Fig. 5f).

ANG siRNA affects the expression of apoptosis related proteins and AKT/mTOR signaling pathway molecules in tumor xenograft tissue

Impact of ANG siRNA on RI, p-Akt, p-GSK3β, p-mTOR, p-4E-BP1 and p-p70 S6 Kinase as well as the expression of apoptosis-related proteins in tumor xenograft tissue were detected by immunohistochemical assays. The T24-siANG group showed higher expression of RI, Bax and cleaved Caspase3 (Fig. 6), as well as lower expression of ANG, p-Akt, p-GSK3β, p-mTOR, p-4E-BP1 and p-p70 S6 Kinase compared with the control groups (Fig. 7). These results were consistent with assays in vitro and further proved the view that down-regulating ANG could inhibit the growth and induce apoptosis in human bladder cancer cells through regulating AKT/mTOR signaling pathway.

Fig. 5 Down-regulating ANG suppresses tumor growth and spontaneous lung metastasis of mouse xenograft model. 2×10^5 tumor cells including the five groups were respectively injected subcutaneously into the backs of the BALB/C nude mice. After 4 weeks, the mice were sacrificed. The tumors and lungs were isolated, weighed, and photographed. **a** Representative images of the tumor of BALB/C nude mice and xenograft tumor. **b** Tumor weight analysis. The tumors in ANG siRNA group were much smaller compared with control group. **c** Microvessel density analysis. The microvessels were randomly counted from 10 different fields under microscope (×200 magnification) corresponding to areas with the highest density of vessels on HE sections. **d** HE staining of tumor sections. *Arrows* indicate microvessels. **e** HE staining of lung sections. T24-siANG cells group markedly suppressed spontaneous lung metastasis without metastatic tumor cells in the lung, compared with the other control groups. *Arrows* show invasive tumor cells in lung. **f** Immunohistochemical staining with an antibody against CD31 antigen of vascular endothelial cells. Immunofluorescent and Histochemical study demonstrated that numerous microvessels could be seen among the tumors of the BALB/C nude mice injected with control cells. In contrast, microvessels were few or absent in the tumor of the mice injected T24-siANG

Discussion

Angiogenin, a 14.2-kDa polypeptide member of the RNase A superfamily, is an angiogenic protein that has been reported to be upregulated and associated with poor prognosis in some human cancers. The mechanisms through which aberrant ANG levels promote specific steps in tumor progression are unknown. In addition, structural and functional analyses reveal that the 123-residue protein contains a ribonucleolytic active site, a receptor binging site and a nuclear localization sequence (NLS), which might be involved in some unknown biological functions (Li et al. 2011). It has been known that the production of ribosomal proteins is mediated by the AKT-mTOR pathway, and the production of rRNAs is likely mediated by ANG (Wei et al. 2011). But, the signal transduction pathway triggered by ANG-Receptor interaction is currently unknown as the ANG receptor has not been fully confirmed. The exact molecular mechanisms by which ANG could promote tumor growth and metastasis remained unclear so far. Almost no investigation of ANG involving in growth and metastasis of bladder cancer cells via AKT/mTOR signaling pathway is reported.

To further elucidate the biological function of ANG, here, we constructed ANG siRNA plasmids that transfected into human bladder T24 cell. The significant findings in the present study are that highlight a pivotal role for ANG in tumor growth and metastasis by regulating AKT/mTOR signaling pathway. Firstly, the experiment demonstrated that down-regulating ANG could obviously change cell morphology,regulate cell cycle, inhibit the cell proliferation and induce cell apoptosis. Apoptosis is a tightly regulated form of programmed cell death involving a series of biochemical events that leads to a variety of morphological changes, such as condensation of chromatin, nuclear fragmentation, and apoptotic bodies, were considered as the most reliable markers of apoptosis (Malla et al. 2010), which were observed in the T24-siANG cell group by the Hoechst 33342 and HE staining. We also detected the occurrence of apoptosis with TUNEL assay, as shown in Fig. 3. The number of Tunel-positive cells significantly increased in T24-siANG cells. Flow cytometry analysis further indicated that about 57.91 % of counted cells became apoptotic in T24-siANG cells using Annexin V-FITC apoptosis detection. Furthermore, key apoptosis-related proteins have also presented significant changes, Bcl-2 was distinctly downregulated and Bax was obviously increased in T24-siANG cells group; down- regulating ANG promoted the cleavage activation of procaspase-3 and increasing of caspase-3 expression. Ibaragi et al. and Yuan et al. reported that ANG is important in regulating rRNA transcription in cells. ANG has been shown to undergo nuclear translocation in both cancer cells and endothelial cells where it stimulates rRNA transcription, a rate-limiting step in protein translation and cell proliferation (Ibaragi et al. 2009a, b; Yuan et al. 2009). Paudel et al. showed that silencing ANG or inhibiting its nuclear translocation resulted in the apoptosis and cell cycle regulation of cells latently infected with KSHV. Our experiment results were consistent with these researches (Paudel et al. 2012).

Secondly, in this study, we investigated several important target molecules to evaluate the effect of ANG siRNA on AKT/mTOR signaling pathway. The results demonstrated that down-regulation of ANG could inhibit phosphorylation of Akt,GSK3β and mTOR in bladder cancer

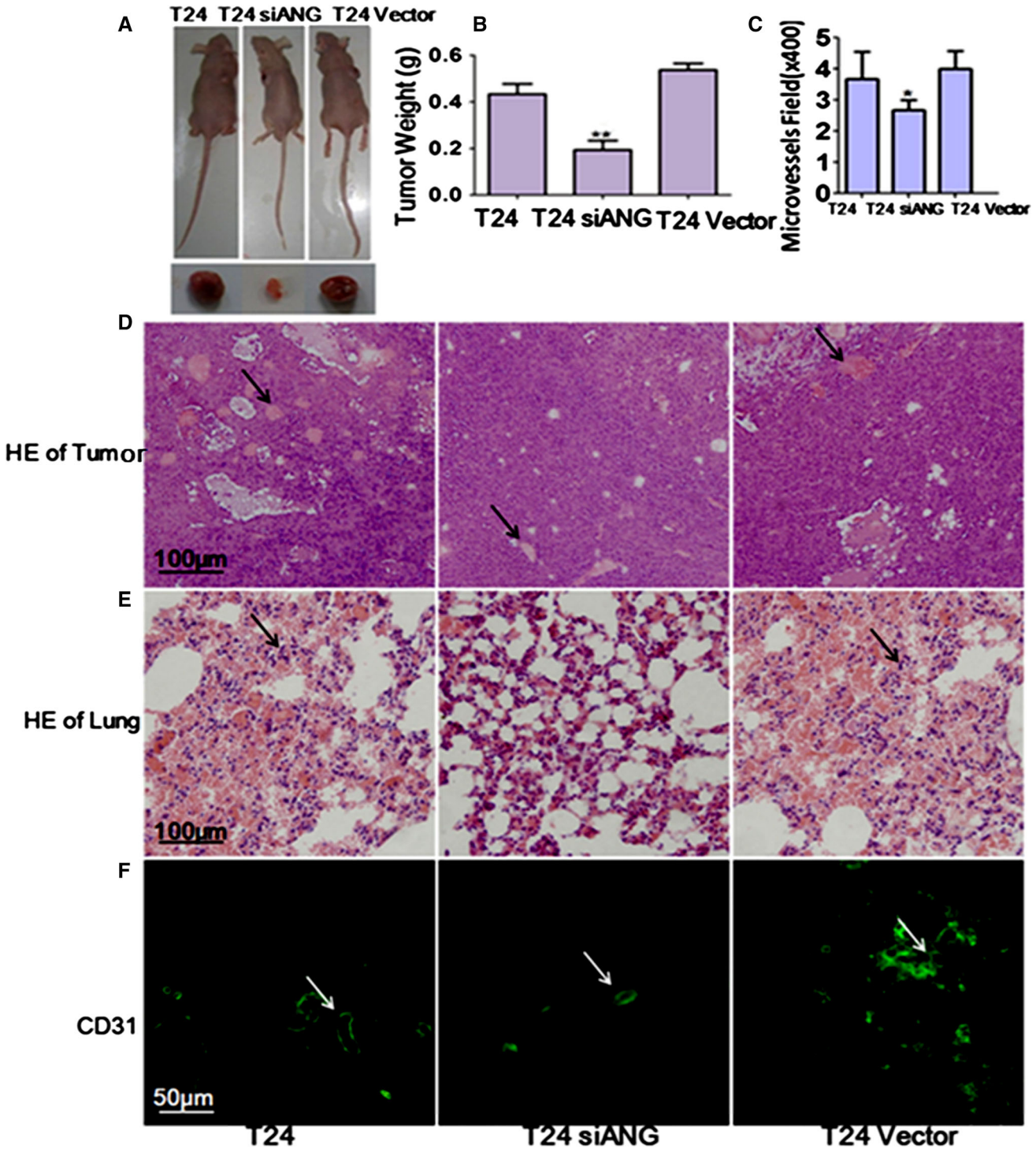

cells in vivo and vitro. Consistently, there is a crosstalk between ANG and AKT pathways. For example, ANG activates AKT, and activated AKT in turn stimulates nuclear translocation of ANG. The production of ribosomal proteins is mediated by the AKT-mTOR pathway. mTOR plays an important role in PI3K- and AKT-dependent oncogenesis. The mTOR acts as a downstream effector for Akt, AKT can directly phosphorylate and activate mTOR (Li and Hu 2010; Reikvam et al. 2013). By promoting the phosphorylation of AKT, which is necessary for angiogenin-induced wound healing migration of HUVE cells and angiogenin-induced angiogenesis in chick chorioallantoic membrane (Kim et al. 2007). (Chang et al. 2013) demonstrate that activation of the PI3K/Akt/mTOR signaling

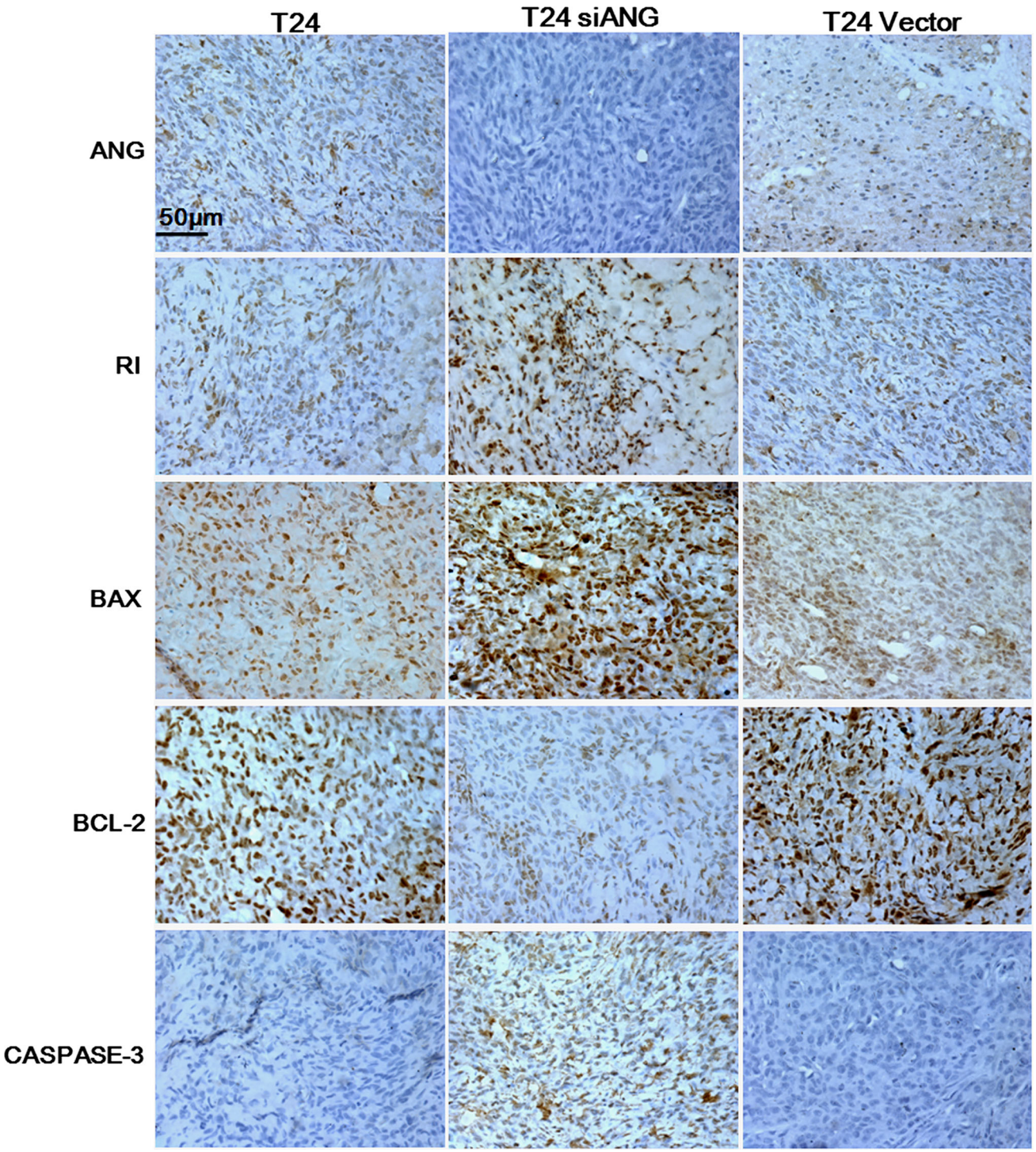

Fig. 6 Down-regulating ANG influences the expressions of apoptosis-related proteins and RI in tumor xenograft tissue. Representative photographs showed that the T24-siANG cell group had a weak brown immunostain for ANG, BCL-2 as well as a strong positive staining for RI, BAX and CASPASE-3 in cytoplasm compared with the control groups respectively (×400 magnification)

pathway which result in cancer cell growth, survival, invasion, DNA repair and metastasis. GSK-3β also plays a role in cell proliferation via regulation of genes involved in cell cycle progression and survival. Likewise, activated AKT also phosphorylate GSK-3 on ser9 (Luo et al. 2014). Our experiment results further supported these findings.

Thirdly, animal experiment manifested that down-regulation of ANG could significantly inhibited the tumor

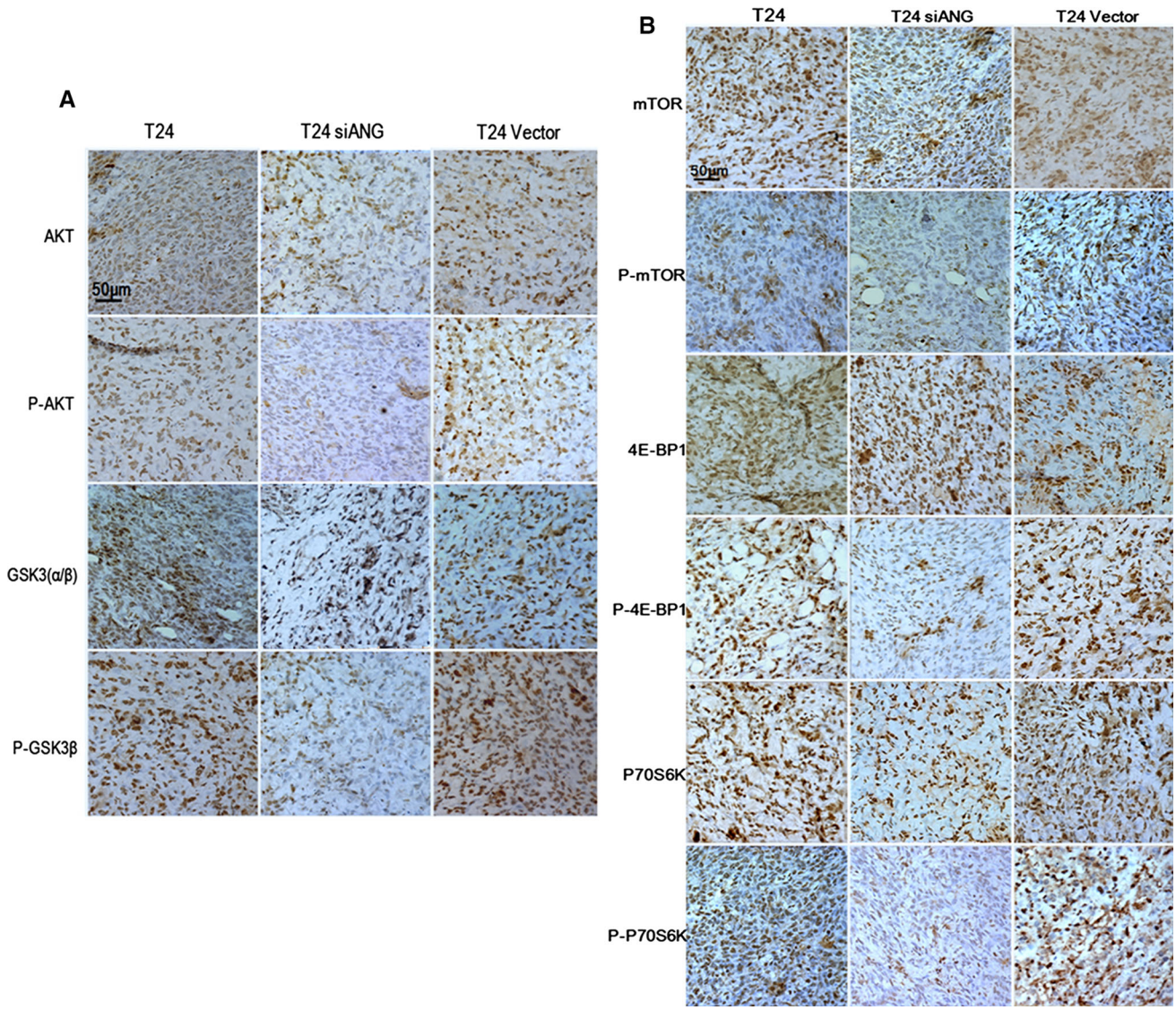

Fig. 7 Down-regulating ANG affects the expressions of AKT/mTOR signaling pathway target molecules with immunohistochemistry in tumor tissue. **a**, **b** Representative photographs showed that the T24-siANG cell group had a weak brown immunostain for p-AKT, p-GSK3β, p-mTOR, p-4E-BP1 and p-p70 S6 Kinase compared with the control groups respectively as well as a similar staining for AKT, GSK3 (α/β), mTOR, 4E-BP1 and p70 S6 Kinase in all groups (×400 magnification)

xenografts growth, tumor angiogenesis and metastasis. Miyake et al. found that targeting ANG in vivo with N65828, a small-molecule inhibitor of the ribonucleolytic activity of human ANG, resulted in the diminution of xenograft tumoral growth through the inhibition of angiogenesis. Ibaragi et al. reported that Neamine inhibited prostate cancer growth by suppressing angiogenin-mediated ribosomal RNA transcription Nilsson et al. (2010); Trouillon et al. (2010). ANG is a prominent angiogenic factor that has been shown to have a dual effect on tumor progression by inducing both angiogenesis and cancer proliferation through stimulating ribosomal RNA transcription in both endothelial cells and cancer cells (Sheng et al. 2014). Compelling evidence indicates that ANG activity is necessary for other angiogenic factors to induce angiogenesis. ANG-induced rRNA transcription appears to be a common down-stream event of tumor angiogenesis. Thus, ANG inhibitors have been shown to inhibit not only ANG-induced angiogenesis but also those induced by other angiogenic factors including VEGF, FGF, and EGF. ANG inhibitors would therefore have a profound effect in inhibiting tumor angiogenesis (Pizzo et al. 2013; Zhu et al. 2013). It is well known that angiogenesis is necessary for the growth and metastasis of tumors. Solid tumor growth often requires vascular remodeling including vessel regression, neovascularization and vascularization to

provide adequate oxygen and nutrients to proliferating cells and avoid necrosis (Muramatsu et al. 2010). In addition, we also explored RI expression and the possibility of colocalization of ANG with RI. The results indicated that down-regulating ANG distinctly increased RI expression in both cells and tissue, ANG and RI has a colocalization, which suggest the two genes might have some interaction or related function, and further research on the relationship between them being carried out in our laboratory. Human ribonuclease inhibitor (RI) is a cytoplasmic acidic protein possibly involved in biological functions other than the inhibition of RNase A and ANG activities. The recent investigation demonstrated that over-expression of RI could inhibit tumor-induced angiogenesis as well as inhibit tumor growth induce cell apoptosis in T24 cells (Yao et al. 2013). We also recently reported that down-regulating RI promoted tumorigenesis and metastasis of bladder cancer (Xiong et al. 2014). Our late experiments showed that up-regulating RI negatively regulated ANG expression in both cells and tissue, and that RI could combine and interact with ANG, which suggest RI might serve to regulate the biological activity of ANG in vivo. We speculate that the RI might bind directly with intracellular ANG to block active center of ribonuclease of ANG and prevent the nuclear translocation of ANG, which result in inhibition of rRNA transcription promotion and other functions of ANG (Li et al. 2014).

In conclusion, our current data reveal a better understanding of the mechanisms underlying the role of ANG in cell proliferation and tumor growth when it was knocked down for the first time in bladder cancer cells. These findings suggest that ANG play a pivotal role in the development of bladder cancer through regulating AKT/mTOR signaling pathway. We believe that ANG could be a good diagnostic and therapeutic target for controlling bladder cancer. However, full elucidation of the mechanism of action of ANG in regulating growth and survival would need identification of ANG receptor and its signaling pathways.

Acknowledgments This work was supported by the National Natural Science Foundation of China (81172424 and 81372203).

Conflict of interest The authors declare no conflict of interest.

References

Chang L, Graham PH, Hao J, Ni J, Bucci J, Cozzi PJ et al (2013) Acquisition of epithelial-mesenchymal transition and cancer stem cell phenotypes is associated with activation of the PI3K/Akt/mTOR pathway in prostate cancer radioresistance. Cell Death Dis 4:e875

Fett JW, Strydom DJ, Lobb RR, Alderman EM, Bethune JL, Riordan JF et al (1985) Isolation and characterization of angiogenin, an angiogenic protein from human carcinoma cells. Biochemistry 24:5480–5486

Ibaragi S, Yoshioka N, Li S, Hu MG, Hirukawa S, Sadow PM et al (2009a) Neamine inhibits prostate cancer growth by suppressing angiogenin-mediated rRNA transcription. Clin Cancer Res 15:1981–1988

Ibaragi S, Yoshioka N, Kishikawa H, Hu JK, Sadow PM, Li M et al (2009b) Angiogenin-stimulated rRNA transcription is essential for initiation and survival of AKT-induced prostate intraepithelial neoplasia. Mol Cancer Res 7:415–424

Ivanov P, Emara MM, Villen J, Gygi SP, Anderson P (2011) Angiogenin-induced tRNA fragments inhibit translation initiation. Mol Cell 43:613–623

Janku F, Wheler JJ, Westin SN, Moulder SL, Naing A, Tsimberidou AM et al (2012) PI3K/AKT/mTOR inhibitors in patients with breast and gynecologic malignancies harboring PIK3CA mutations. J Clin Oncol 30:777–782

Janku F, Wheler JJ, Naing A, Falchook GS, Hong DS, Stepanek VM et al (2013) PIK3CA mutation H1047R is associated with response to PI3K/AKT/mTOR signaling pathway inhibitors in early-phase clinical trials. Cancer Res 73:276–284

Jemal A, Bray F, Center MM, Ferlay J, Ward E, Forman D (2011) Global cancer statistics. CA: A Cancer J Clin 61:69–90

Kieran D, Sebastia J, Greenway MJ, King MA, Connaughton D, Concannon CG (2008) Control of motoneuron survival by angiogenin. J Neurosci 28:14056–14061

Kim HM, Kang DK, Kim HY, Kang SS, Chang SI (2007) Angiogenin-induced protein kinase B/Akt activation is necessary for angiogenesis but is independent of nuclear translocation of angiogenin in HUVE cells. Biochem Biophys Res Commun 352:509–513

Li S, Hu GF (2010) Angiogenin-mediated rRNA transcription in cancer and neurodegeneration. Int J Biochem Mol Biol 1:26–35

Li S, Hu GF (2012) Emerging role of angiogenin in stress response and cell survival under adverse conditions. J Cell Physiol 227:2822–2826

Li S, Ibaragi S, Hu GF (2011) Angiogenin as a molecular target for the treatment of prostate cancer. Curr Cancer Ther Rev 7:83–90

Li L, Pan XY, Shu J, Jiang R, Zhou YJ, Chen JX (2014) Ribonuclease inhibitor up-regulation inhibits the growth and induces apoptosis in murine melanoma cells through repression of angiogenin and ILK/PI3K/AKT signaling pathway. Biochimie 103:89–100

Liu P, Cheng H, Roberts TM, Zhao JJ (2009) Targeting the phosphoinositide 3-kinase pathway in cancer. Nat Rev Drug Discov 8:627–644

Luo F, Burke K, Kantor C, Miller RH, Yang Y (2014) Cyclin-dependent kinase 5 mediates adult OPC maturation and myelin repair through modulation of akt and gsk-3β signaling. J Neurosci 34:10415–10429

Malla R, Gopinath S, Alapati K, Gondi CS, Gujrati M, Dinh DH et al (2010) Downregulation of uPAR and cathepsin B induces apoptosis via regulation of Bcl-2 and Bax and inhibition of the PI3K/Akt pathway in gliomas. PLoS One 5:e13731

Muramatsu M, Yamamoto S, Osawa T, Shibuya M (2010) Vascular endothelial growth factor receptor-1 signaling promotes mobilization of macrophage lineage cells from bone marrow and stimulates solid tumor growth. Cancer Res 70:8211–8221

Nilsson UW, Abrahamsson A, Dabrosin C (2010) Angiogenin regulation by estradiol in breast tissue: tamoxifen inhibits angiogenin nuclear translocation and antiangiogenin therapy reduces breast cancer growth in vivo. Clin Cancer Res 16:3659–3669

Paudel N, Sadagopan S, Chakraborty S, Sarek G, Ojala PM, Chandran B (2012) Kaposi's sarcoma-associated herpesvirus latency-associated nuclear antigen interacts with multifunctional angiogenin to utilize its antiapoptotic functions. J Virol 86:5974–5991

Pizzo E, Sarcinelli C, Sheng J, Fusco S, Formiggini F, Netti P et al (2013) Ribonuclease/angiogenin inhibitor 1 regulates stress-induced subcellular localization of angiogenin to control growth and survival. J Cell Sci 126:4308–4319

Reikvam H, Nepstad I, Bruserud Ø, Hatfield KJ (2013) Pharmacologic targeting of the PI3K/mTOR pathway controls release of angioregulators from primary human acute myeloid leukemia cells and their neighboring stromal cells. Oncotarget 4:830–843

Rosser CJ, Ross S, Chang M, Dai Y, Mengual L, Zhang G et al (2013) Multiplex protein signature for the detection of bladder cancer in voided urine samples. J Urol 190:2257–2262

Sheng J, Yu W, Gao X, Xu Z, Hu GF (2014) Angiogenin stimulates ribosomal RNA transcription by epigenetic activation of the ribosomal DNA promoter. J Cell Physiol 229:521–529

Suriano F, Altobelli E, Sergi F, Buscarini M (2013) Bladder cancer after radiotherapy for prostate cancer. Rev Urol 15:108–112

Trouillon R, Kang DK, Park H, Chang SI, O'Hare D (2010) Angiogenin induces nitric oxide synthesis in endothelial cells through PI-3 and Akt kinases. Biochemistry 49:3282–3288

Urquidi V, Goodison S, Kim J, Chang M, Dai Y, Rosser CJ (2012) Vascular endothelial growth factor, carbonic anhydrase 9, and angiogenin as urinary biomarkers for bladder cancer detection. Urology 79(1185):e1–6

Wei S, Gao X, Du J, Su J, Xu Z (2011) Angiogenin enhances cell migration by regulating stress fiber assembly and focal adhesion dynamics. PLoS One 6:e28797

Xiong D, Liou Y, Shu J, Li D, Zhang L, Chen J (2014) Down-regulating ribonuclease inhibitor enhances metastasis of bladder cancer cells through regulating epithelial-mesenchymal transition and ILK signaling pathway. Exp Mol Pathol 96:411–421

Yao X, Li D, Xiong DM, Li L, Jiang R, Chen JX (2013) A novel role of ribonuclease inhibitor in regulation of epithelial-to-mesenchymal transition and ILK signaling pathway in bladder cancer cells. Cell Tissue Res 353:409–423

Yoshioka N, Wang L, Kishimoto K, Tsuji T, Hu GF (2006) A therapeutic target for prostate cancer based on angiogenin-stimulated angiogenesis and cancer cell proliferation. Proc Natl Acad Sci USA 103:14519–14524

Yuan Y, Wang F, Liu XH, Gong DJ, Cheng HZ, Huang SD (2009) Angiogenin is involved in lung adenocarcinoma cell proliferation and angiogenesis. Lung Cancer 66:28–36

Zhu J, Sheng J, Dong H, Kang L, Ang J, Xu Z (2013) Phospholipid scramblase 1 functionally interacts with angiogenin and regulates angiogenin-enhanced rRNA transcription. Cell Physiol Biochem 32:1695–1706